Coupling Analysis Between Ecological Environment Change and Urbanization Process in the Middle Reaches of Yangtze River Urban Agglomeration, China

Can Li, Tao Chen, *Senior Member, IEEE*, Kun Jia, and Antonio Plaza, *Fellow, IEEE*

***Abstract*—In 2014, the Chinese government upgraded the construction of the "Yangtze River Economic Belt" to a national strategy, and the Urban Agglomeration in the Middle Reaches of the Yangtze River (UAMRYR) has experienced a rapid urbanization process. The study adopts remote sensing ecological index, compound night light index, extraction of built-up areas, urbanization and ecological environment quality (EEQ) coordinated development coupling model to assess the EEQ, urbanization and the relationship between them in the UAMRYR during the period spanning 2013 to 2021. The results show that: 1) between 2013 and 2021, the EEQ of UAMRYR exhibited a notable decline in 2015, followed by a gradual but consistent improvement; 2) the urbanization level within UAMRYR demonstrated a steady increase throughout the same period from 2013 to 2021; 3) over the course of 2013 to 2021, a majority of the cities had transitioned from a state of low coordination to medium coordination. In addition, the urban dynamic development stage of the three provincial capitals progressed from a state of low coordination to coordinated development, with the entire coordinated development system on the verge of entering an advanced stage of extreme development. The experimental results were used to classify the cities in the UAMRYR into five types, and the reasons restricting the development of the urban agglomerations were analyzed. It also briefly touches upon the influence of extreme climate events on the EEQ. These findings hold significant importance in the endeavor to promote urbanization while simultaneously optimizing the EEQ, thus contributing to the construction of resilient cities.**

***Index Terms*—Coordinated development, ecological environment quality, urban agglomeration, urbanization.**

Manuscript received 4 March 2024; revised 17 May 2024; accepted 18 June 2024. Date of publication 26 June 2024; date of current version 8 July 2024. This work was supported in part by the National Natural Science Foundation of China under Grant 62371430 and Grant 62071439, in part by the Open Fund of State Key Laboratory of Remote Sensing Science under Grant OFSLRSS-202207, in part by the Open Fund of Badong National Observation and Research Station of Geohazards under Grant BNORSG-202302, in part by the Opening Fund of the Key Laboratory of National Geographic Census and Monitoring, Ministry of Natural Resources under Grant 2023NGCM11, and in part by the Opening fund of State Key Laboratory of Geohazard Prevention and Geoenvironment Protection (Chengdu University of Technology) under Grant SKLGP2022K016. *(Corresponding author: Tao Chen.)*

Can Li is with the School of Geophysics and Geomatics, China University of Geosciences, Wuhan 430074, China (e-mail: can.li@cug.edu.cn).

Tao Chen is with the School of Geophysics and Geomatics, China University of Geosciences, Wuhan 430074, China, also with the State Key Laboratory of Remote Sensing Science, Faculty of Geographical Science, Beijing Normal University, Beijing 100875, China, also with the Badong National Observation and Research Station of Geohazards, China University of Geosciences, Wuhan 430074, PR China, and also with the Key Laboratory of National Geographic Census and Monitoring, Ministry of Natural Resources, Wuhan 430079, PR China (e-mail: taochen@cug.edu.cn).

Kun Jia is with the State Key Laboratory of Remote Sensing Science, Faculty of Geographical Science, Beijing Normal University, Beijing 100875, China, and also with the Beijing Engineering Research Center for Global Land Remote Sensing Products, Faculty of Geographical Science, Beijing Normal University, Beijing 100875, China (e-mail: jiakun@bnu.edu.cn).

Antonio Plaza is with the Hyperspectral Computing Laboratory, Department of Technology of Computers and Communications, Escuela Politécnica, University of Extremadura, 10071 Cáceres, Spain (e-mail: aplaza@unex.es).

Digital Object Identifier 10.1109/JSTARS.2024.3419154

I. Introduction

As the economy continues to flourish and urbanization advances unabated, the encroachment of ecological space due to urban expansion, industrial pollution, and heightened socio-economic activities has escalated [1]. Simultaneously, the rapid urban sprawl has transformed once-vital forested areas, arable land, farmlands, and lakes into commercial and industrial zones. This transformation has considerably diminished vegetation cover and ecological efficacy, exacerbating issues like vegetation depletion [2], soil erosion [3], and the urban heat island [4]. Rapid urbanization inevitably disturbs and even destroys ecological environment quality (EEQ), at the same time, the degradation of EEQ can also constrain urbanization and its sustainable development. Ecosystems across the globe are facing with unprecedented challenges [5], [6], simultaneously jeopardizing the sustainable future of cities [7], [8]. Therefore, a comprehensive analysis and evaluation of the nexus between EEQ and the urbanization process, maintaining balanced ecosystem development, and ensuring the proper functioning of urban ecosystem services are crucial for promoting sustainable urban development in different geographic regions.

Currently, the EEQ monitoring and evaluation approaches primarily center around two key aspects: 1) Single-indicator evaluation methods. Examples of such indicators include the air quality index (AQI) [9] and the water quality index (WQI) [10]. 2) integrated indicator evaluation method. Examples include the environmental quality index (EQI) utilized by the U.S. Environmental Protection Agency [11] and the Ecological Index (EI) featured in China's EEQ Standard [12]. These comprehensive approaches offer a more thorough assessment of environmental conditions [13], [14]. The evaluation of urbanization is commonly done using comprehensive indicators. Because

of urban constitutes an intricate system encompassing various city subsystems, including population, economy, land use, and societal factors [15], [16]. In the 1970s, Japan introduced the Urban Growth Force Coefficient method, employing 10 composite indexes to gauge urbanization levels [17]. Subsequently, in 2002, the United Nations introduced the Urban Development Index, comprising 12 indicators to evaluate urbanization levels [18]. Many complex problems are encountered in the process of evaluating and analyzing EEQ and urbanization. With the development of remote sensing technology, its advantages—such as speed, precision, large coverage, and substantial data volume—provide a robust data source for evaluating EEQ and urbanization. The powerful spatial data processing and analysis capabilities of geographic information technology ensure reliable subsequent spatial analysis. Consequently, numerous evaluation methods based on remotely sensed data have emerged. These include the remote sensing ecological index (RSEI) [19] for evaluating EEQ and the compound night light index (CNLI) [20] for assessing urbanization levels. These methods provide comprehensive, scientific, and accurate approaches to evaluating of EEQ and urbanization.

Since the beginning of the last century, scholars have worked to explore the relationship between the EEQ and urbanization. Kenneth Boulding is credited with coining the term "ecological economics" in 1966 [21]. In 1972, scholars in the United States constructed a dynamic system model, elucidated the impact of the development of primary and secondary industries on population, resources, and the environment [22]. Panayotou and Theodore [23] introduced the Environmental Kuznets Curve, this curve illustrates an inverted "U" shape, signifying the complex interplay between environmental quality and per capita income. These foundational studies have paved the way for further exploration and analysis in this critical field of study. With a deeper understanding of the scientific concept of development, the coupled evaluation method has emerged as an effective tool for assessing the mutual influence and overall balanced development of two or more systems. This method has been widely applied across various fields [24], [25], [26]. Qiao and Fang [27] analyzed the interactive coupling dynamics between natural and human elements within urban agglomeration systems and formulated a spatial-temporal coupling dynamics model. Liu et al. [28] developed a coupling degree model between urbanization and the EEQ, building upon the concept of synergy and elaborating on the meaning of their interdependence. Zhang et al. [29] used geoprobes to analyze key factors affecting CCD. The coupled development model provides more specific evaluation criteria in evaluating the relationship between EEQ and urban development. It quantifies the coordinated development between these two aspects, providing clearer and more accurate data and theoretical support for sustainable urban development.

The Middle Reaches of the Yangtze River (UAMRYR) is an important part of the Yangtze River Economic Belt (YRB), and the strategy of building the YRB was formally determined as a national strategy in 2014 [30], and UAMRYR, as one of the three major city clusters in the YRB, has also experienced a rapid urbanization process [31]. Therefore, this study analyzes the EEQ, urbanization level, and the relationship between EEQ and urbanization level in the urban agglomeration in the middle reaches of the Yangtze River from 2013 to 2021 by using remote sensing image data, nighttime light data, and the model of coupled development of EEQ and urbanization.

The main contributions of this study are: 1) Utilizing urban agglomeration development policy as a foundation, we employed two relational analysis methods to examine the relationship between EEQ, urbanization level, and dynamic development stages of cities. 2) Based on our analyses, we categorized cities within urban agglomerations and proposed development directions and challenges for each category.

The rest of this article is organized as follows: Section II gives a description of the study area and and the methods principles used in this article. Section III presents the results of the experiment and analyzes them. Discussion of experimental results are given in Section IV. Finally, Section V concludes this article.

II. Materials and Methods

A. Study Area

UAMRYR is located in the central part of the YRB, spanning from 110°45′-118°21′ E and 26°03′-32°38′ N. Its center city is Wuhan, with Changsha and Nanchang as its subcenters. These three provincial capital cities form a triangular geographic complex (see Fig. 1). The elevation within UAMRYR ranges from 20 to 3105 m, and the region is predominantly characterized by fertile plains. It boasts a rich diversity of species, abundant water resources, and a complex network of interconnected lakes and wetlands, playing a vital role as an ecological barrier within the Yangtze River Basin. Furthermore, UAMRYR forms the foundation for the development of urban clusters surrounding Wuhan in Hubei province, the Changsha–Zhuzhou–Xiangtan city group in Hunan province, and clusters around Poyang Lake in Jiangxi province.

B. Data Source and Preprocessing

In this study, we used the Google Earth Engine (GEE) platform to obtain Landsat 8 data for June to September of each year from 2013 to 2021 to calculate the RSEI. Vegetation growth is more stable during this period, which can reduce the influence of climatic transitions on the experimental results. The remote sensing data procured from GEE were undergone radiometric calibration and atmospheric correction. Subsequent preprocessing steps involved regional filtering, de-clouding, water masking, and median synthesis operations. Cloud removal was performed by acquiring the quality assessment (QA) band of the surface reflectance (SR) data and setting the values of both cloudShadowBitMask and cloudsBitMask to 0. Water bodies in the study area were removed using the Modified Normalized Difference Water Index (MNDWI) [32] for the Landsat8 imagery. Even after preprocessing, certain time series and regional gaps in the synthesized remote sensing images were observed. To address this issue, the GEE platform's functionality was employed to interpolate the data's time series spanning the years 2013–2021, resulting in improved data completeness.

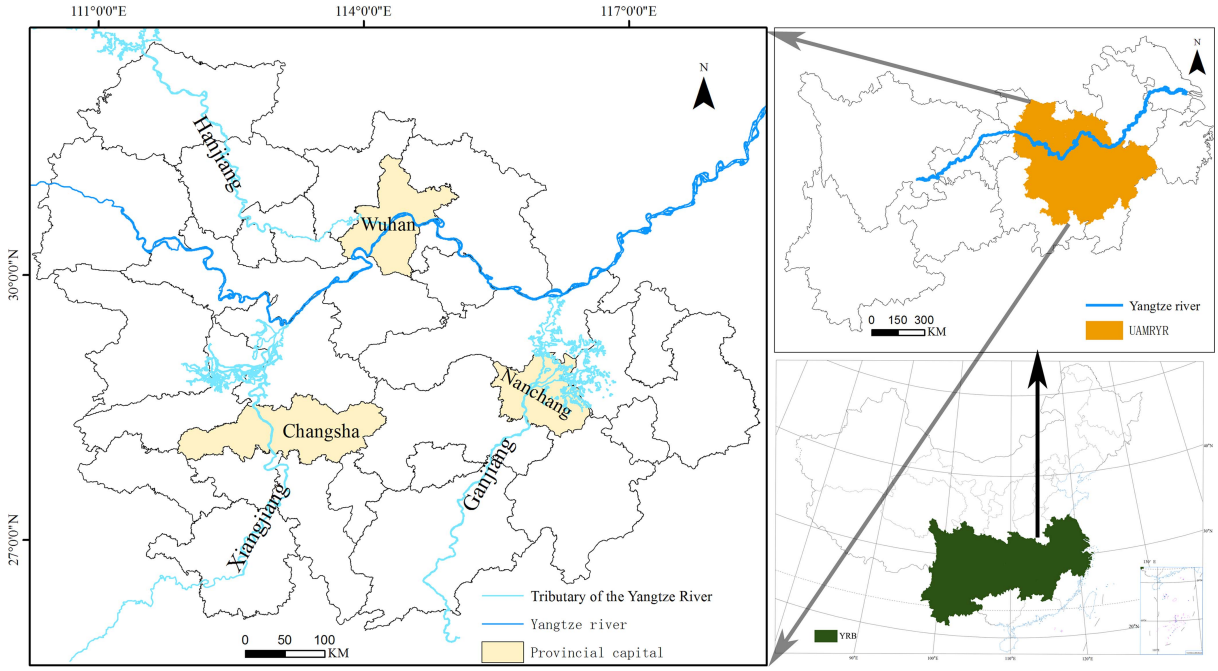

Fig. 1. Location of the study area.

Nighttime light data, as a form of remote sensing information, are intuitive, comprehensive, and efficient, and are widely used in evaluating urbanization levels [33], [34], [35]. For this study, we selected the NPP/VIIRS annual dataset provided by the Earth Observation Group. This dataset offers notable enhancements in light capture sensitivity, the range of light values, and spatial resolution [36], [37]. However, prior to use, background noise was meticulously removed. Drawing from prior experience, all pixel values were sorted in ascending order, with the value at the 99.9th percentile serving as the maximum threshold. Pixels exceeding this threshold were capped at the maximum value. The average value of water body pixels was calculated as the minimum threshold. Pixels corresponding to water bodies and those falling below the minimum threshold were assigned a value of 0 [38]. This method can effectively eliminate the effects of transient light sources and background noise, and correct the light radiation and pixel distribution.

Vector data utilized in this study were sourced from the Center for Resource and Environmental Science and Data. Additional statistical information, such as the green area ratio of built-up areas, was derived from officially published statistical almanacs (see Table I).

TABLE I
DATA USED IN THIS STUDY

Category	Name	Source
Remote sensing data	Landsat 8 OLI/TIRS	Google Earth Engine
Nighttime light data	NPP/VIIRS	Earth Observation Group NOAA/NGDC - Earth Observation Group
Vector data	Administrative boundaries River	www.resdc.cn
Terrain data	Elevation	www.resdc.cn
Statistical data	Size of built-up area Green space ratio in built-up areas	Statistical Yearbook

C. Methods

1) Remote Sensing Ecological Index: Remote Sensing Ecological Index is an ecological index rooted in remote sensing data, was introduced in accordance with the Technical Specification for the Evaluation of Ecologocal Environment Conditions. This approach has been successfully applied in various regions [39], [40], [41], [42]. The RSEI was constructed using principal component analysis (PCA), taking four key indicators closely related to the quality of the natural environment: greenness, humidity, heat, and dryness. The RSEI was obtained by standardizing the first principal component after principal component analysis, and the calculation method is shown in (1).

$$\mathrm{RSEI} = \mathrm{PCA}\left(\mathrm{Greenness}, \mathrm{Wetness}, \mathrm{Heat}, \mathrm{Dryness}\right). \quad (1)$$

The greenness factor is replaced by NDVI, as shown in (2), which is the most widely used vegetation index.

$$\mathrm{NDVI} = \left(\rho_5 - \rho_4\right) / \left(\rho_5 + \rho_4\right). \quad (2)$$

The wetness factor is represented by the humidity component of the tassel-cap transform, which is expressed by (3), and is

closely related to the EEQ.

$$\mathrm{WET} = 0.1511\rho_2 + 0.1973\rho_3 + 0.3283\rho_4 + 0.3407\rho_5 - 0.7117\rho_6 - 0.4599\rho_7. \quad (3)$$

The dryness factor is expressed using the normalized difference building index (NDBSI), which is a combination of the bare soil index (SI) (4), and the building index (IBI) (5). The calculation of RSEI is shown in (6)

$$\mathrm{SI} = \frac{[(\rho_6 + \rho_4) - (\rho_5 + \rho_2)]}{[(\rho_6 + \rho_4) + (\rho_5 + \rho_2)]} \quad (4)$$

$$\mathrm{IBI} = \frac{\frac{2\rho_6}{\rho_6+\rho_5} - \left[\frac{\rho_5}{\rho_5+\rho_4} + \frac{\rho_3}{\rho_3+\rho_6}\right]}{\frac{2\rho_6}{\rho_6+\rho_5} + \left[\frac{\rho_5}{\rho_5+\rho_4} + \frac{\rho_3}{\rho_3+\rho_6}\right]} \quad (5)$$

$$\mathrm{NDBSI} = (\mathrm{SI} + \mathrm{IBI})/2. \quad (6)$$

The heat factor is expressed using the land surface temperature (LST), which is calculated using the atmospheric correction method (7)

$$\mathrm{LST} = t/[1 + \lambda * t/ln\varepsilon] \quad (7)$$

$$L = \mathrm{gain} * \mathrm{DN} + \mathrm{bias} \quad (8)$$

$$t = K_2/\ln(K_1/L_i + 1) \quad (9)$$

where ρ_i(i = 1,2,3 ……)is the reflectance of each band of Landsat 8 OIL. ε is the surface specific emissivity, L is the radiance value of the pixel at the sensor for the thermal infrared band, t is the value of luminance temperature, DN is the value of gray scale of the pixel, gain, bias are the value of gain and bias for the thermal infrared band. K_1, K_2 are calibration parameters.

2) Compound Night Light Index: The compound night light index is a lighting metric derived from nighttime light data, which involves the calculation of two key parameters: the mean light intensity (MLI) and the light area percentage (LAP). The calculation process is outlined as follows:

$$\mathrm{CNLI} = \mathrm{MLI} * \mathrm{LAP} \quad (10)$$

$$\mathrm{MLI} = \sum_{i=1}^{n} C_i * DN_i / \sum_{i=1}^{n} C_i * n \quad (11)$$

$$\mathrm{LAP} = \mathrm{Area}_{\mathrm{light}}/\mathrm{Area}\,. \quad (12)$$

where the value of I is obtained by removing outliers and noise from the VIIRS nighttime light data, resulting in a value of n = 92. DN_i represents the pixel value, C_i signifies the number of pixels with the value of DN_i, $\mathrm{Area}_{\mathrm{light}}$ denotes the lighted area, and area denotes the total area of the study area.

3) Urbanization and EEQ Coordinated Development Coupling Model:

a) Quantitative analysis model: The coupled coordination degree model is used to analyze the level of coordinated development between systems, and the calculation formula is shown as follows:

$$C = \frac{2(U*E)^{\frac{1}{2}}}{(U+E)} \quad (13)$$

$$T = a*U + b*E \quad (14)$$

$$D = (C*T)^{1/2} \quad (15)$$

where C is the degree of coupling, U, E correspond to the compound night light index and remote sensing ecological index, respectively. D is the degree of coupling coordination. T denotes the composite index for urbanization and EEQ coordination. a, b are parameters to be determined, and they must satisfy the condition that $a + b = 1$. In this study, both the ecological quality and the urbanization process are considered equally important. Hence, for this study, a, b are both set to 0.5 to reflect their equal importance.

Based on the previous division methods [43], [44] and the specifics of this study, we chose the current division method. The intervals are divided as follows: When $0 \le D \le 0.4$, it indicates a low level of coordinated coupling, When $0.4 \le D \le 0.5$, it reflects a medium level of coordinated coupling. When $0.5 \le D \le 0.8$, it signifies a high level of coordinated coupling. When $0.8 \le D \le 1$, it represents an extremely high level of coordinated coupling.

b) Model of dynamic development over time: The urbanization process can be seen as a developmental journey marked by comprehensive coordination and interactive influence across various levels of urbanization and the EEQ. Accordingly, drawing on the idea of system evolution in system theory, a dynamic coupling model between these two elements is developed. It aims to analyze the dynamic evolution and coupling state within the composite system formed by urbanization and the EEQ.

Both urbanization and ecological change are characterized by nonlinear processes, and their respective evolutionary equations can be formulated as follows:

$$dx(t)/dt = f(x_1, x_2, \ldots x_n)\,. \quad (16)$$

This establishes a general function describing the process of urbanization and ecological change

$$f(U) = \sum_{i=1}^{n} a_i * x_i\,, i = 1, 2, \ldots, n \quad (17)$$

$$f(E) = \sum_{j=1}^{n} b_j * y_j\,,\ j = 1, 2, \ldots, n \quad (18)$$

where x, y are the elements in the system and a, b are the weights of the elements.

The evolutionary rates of the two subsystems are obtained as follows, separately:

$$A = df(E)/dt,\ V_A = dA/dt \quad (19)$$

$$B = df(U)/dt,\ V_B = dB/dt. \quad (20)$$

The combined rates of evolution of these two subsystems collectively determine the overall evolutionary state of the entire system

$$\alpha = \mathrm{arc}tg(V_A/V_B)\,. \quad (21)$$

When $-90° < \alpha \le 0°$ (fourth quadrant), the system is in the stage of low-level coordination; when $0° < \alpha \le 90°$ (first

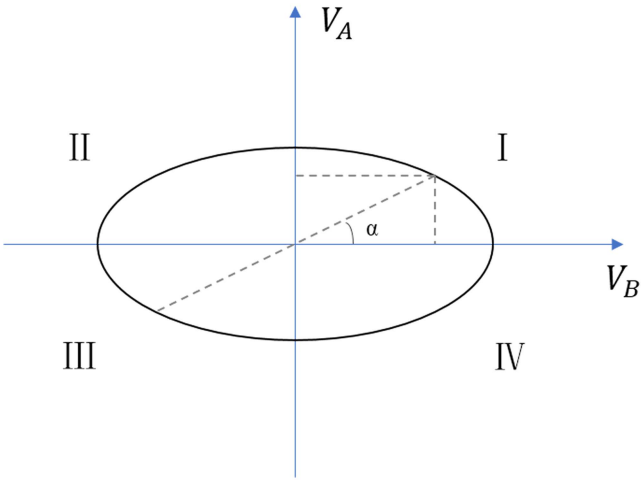

Fig. 2. Evolutionary state.

quadrant), the system is in the stage of coordinated development; when $90° < \alpha \leq 180°$ (second quadrant), the system is in the stage of limiting development; when $-180° < \alpha \leq -90°$ (third quadrant), the system is in the stage of degradation and reorganization, as shown in Fig. 2.

D. Study Framework

In this study, the remote sensing ecological index was firstly calculated in GEE platform using Landsat 8 data to evaluate the EEQ. The compound night light index was calculated from VIIRS/NPP data to evaluate the urbanization process, and also the built-up area was extracted using the nighttime light data to reflect the urban expansion, and the change of the RSEI in the built-up area was counted to reflect the changes in the EEQ in urban construction. Finally, the coupling coordination model and dynamic coupling model are used to calculate the coupling coordination degree and dynamic coupling stage of the city cluster, reflecting the interaction between urbanization and EEQ. According to the results, we analyze the pattern of city development within the city cluster and the direction of city cluster development. The detailed flowchart is shown in Fig. 3.

III. Results and Analysis

A. Trends in Ecological Environment Quality

The results of PCA reveal that greenness and wetness have a positive impact on RSEI, while dryness and heat exert a negative influence on RSEI. Over the period 2013–2021, the contribution of the first principal component is essentially 70%–80%. This indicates that the first principal component effectively captures most of the information and that the RSEI can more accurately reflect the EEQ in the study area. As depicted in Fig. 4, the RSEI for UAMRYR undergoes a fluctuating pattern over the nine-year period, characterized by an initial decrease, followed by an increase, and then a slow decline. Notably, there is a substantial drop in RSEI values in 2015. This decline may be attributed to two main factors. First, 2015 recorded the highest average annual temperature since meteorological records began in 1951, resulting in exceptionally high LST values. Second, the rapid construction following the designation of the YRB as a national strategy in 2014 led to a significant increase in the NDBSI. However, during this period, the WET and the NDVI had not fully recovered from the rapid urbanization. These factors combined led to a significant decrease in RSEI in 2015. After which the concept of coordinated development was emphasized and the EEQ gradually improved.

The distribution of RSEI across each administrative region within the UAMRYR is illustrated in Fig. 5. There is a clear spatial clustering pattern evident in the distribution. This depiction reveals that regions characterized by a higher level of urbanization, such as Wuhan and Nanchang, consistently exhibit significantly lower mean RSEI values than areas with lower levels of urbanization. Notably, Changsha, serving as a provincial capital, consistently maintains a higher RSEI value compared to the other two provincial capitals. In Hubei Province, RSEI values within its administrative districts are generally lower than those in the other two provinces, although Xianning and Yichang in Hubei Province consistently exhibit notably higher RSEI values compared to other regions within the province. Hunan Province, on the other hand, demonstrates a relatively even distribution of RSEI values across its administrative districts, with minimal variation between them. Meanwhile, the southwestern administrative districts of Jiangxi Province consistently feature higher RSEI values than their counterparts in other regions of the province. Overall, regions with higher mean RSEI values tend to be situated on the peripheries of urban agglomerations, and as urbanization progresses, the differences in RSEI between regions are gradually diminishing.

B. Trends in Urbanization Processes

1) Extraction of Nighttime Lights on the Built-Up Area of the City: In this study, the optimal threshold for extracting built-up areas is determined using the statistical data method [45]. The built-up area extents for the three provincial capital cities of Wuhan, Changsha, and Nanchang are extracted for the years 2013 to 2021. The change of built-up area region can reflect the construction process within the city. As can be seen from the Fig. 6, it is evident that the built-up area boundaries of these three provincial capital cities are progressively expanding outward over the study period, and their built-up areas have generally increased in size, with most development occurring along rivers and streams.

There is a clear consistency by comparing with remote sensing images of the same period. This also confirms the reliability of using nighttime light data to assess the urbanization process.

2) CNLI Changes of UAMRYR From 2013 to 2021: In Fig. 7, there is a clear trend of the CNLI for the UAMRYR exhibits a predominantly upward trajectory, indicating a consistent trend of rapid increase. Notably, there is a dip in the CNLI values in 2014, which is likely attributable to a transitional phase resulting from ongoing urban construction activities.

Fig. 8 illustrates that the urbanization levels of Wuhan, Changsha, and Nanchang, the three capital cities within the

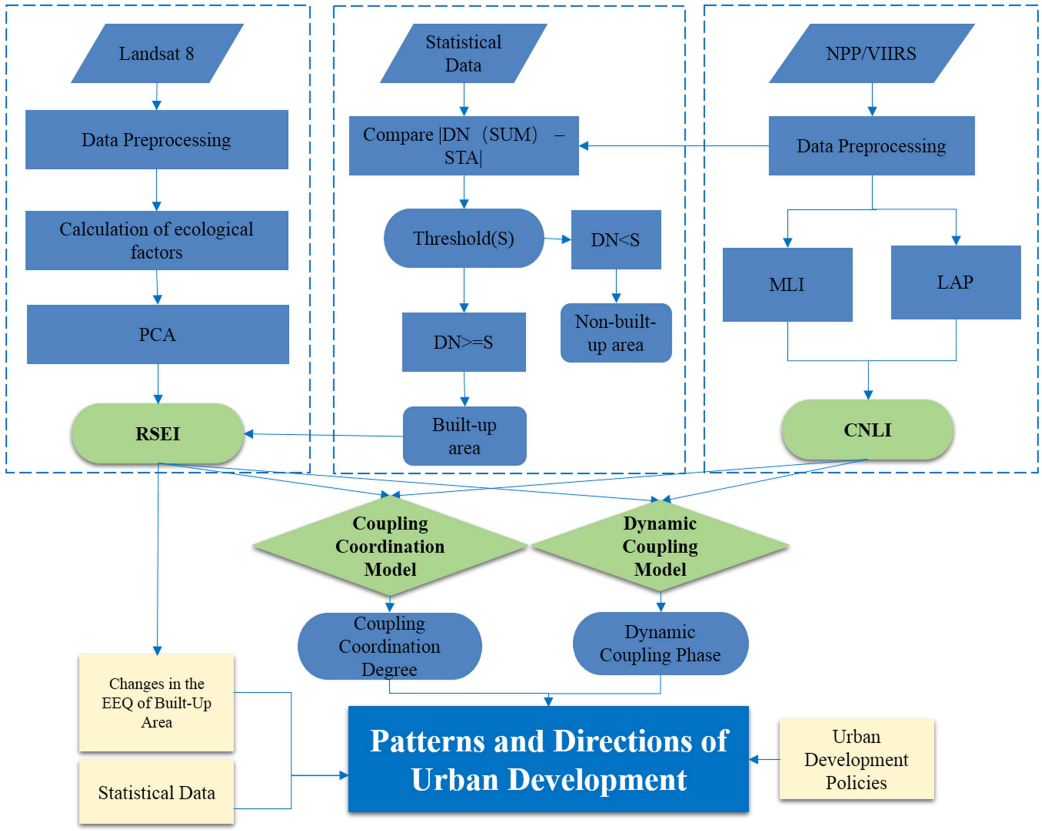

Fig. 3. Flowchart of the proposed framework.

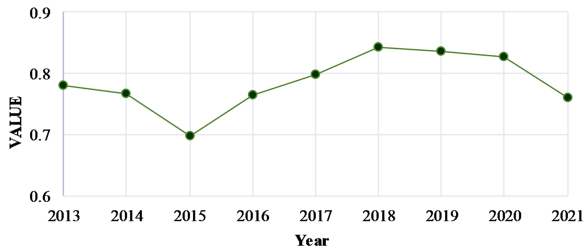

Fig. 4. RSEI changes of UAMRYR from 2013 to 2021.

UAMRYR, consistently surpass those of other regions. Moreover, as urbanization progresses, the mean CNLI values of the surrounding administrative districts, expanding outward from the three capital cities, exhibit a gradual increase. Over time, the CNLI of the central city(wuhan) gradually exceeds that of the two subcenters city. Cities located in proximity to the provincial capitals have experienced more rapid development compared to other urban areas. Examples include Ezhou, situated near Wuhan, and Xiangtan, in close proximity to Changsha. Although Xiangyang and Jingdezhen are located in the periphery of the urban agglomeration, they have a higher level of urban development than the neighboring areas due to the advantages of transportation and cultural tourism.

C. Coupling Coordination Degree Results

1) Coupling Coordination Degree Analysis: It becomes evident that the coupling coordination degree began to decline from 2014, began to rebound in 2016, and stabilized in 2019 from Fig. 9. This pattern is consistent across the three provincial capital cities. Moreover, the coupling coordination degree of the three provincial capital cities consistently exceeds the average value of the entire study area. Notably, Wuhan consistently maintains a higher coupling coordination degree than the other two provincial capital cities.

The urban development of the three provincial capital cities has always maintained a highly coordinated coupling state is shown in Fig. 10.

As the urbanization process advances, the degree of coordination of other cities surrounding the provincial capital cities has been gradually increasing. Furthermore, the range of cities experiencing this increase in coordination extends outward from the three provincial capital cities, indicating a radiating development pattern. By 2021, the majority of cities have transitioned from a low degree of coordination in the coupling state to a medium degree of coordination, underscoring the trend of development radiating from the central cities to the periphery. It is worth noting that compared to Wuhan and Changsha, the cities surrounding Nanchang have exhibited a slower rate of development. In summary, the cities within the UAMRYR can be categorized into five types (see Fig. 11).

Type 1: Central Cities, this category includes Wuhan, Changsha, and Nanchang, the three provincial capitals. They possess more comprehensive city functions, have undergone a more advanced urbanization process compared to other cities, and serve as the core cities within their respective city circles. The central

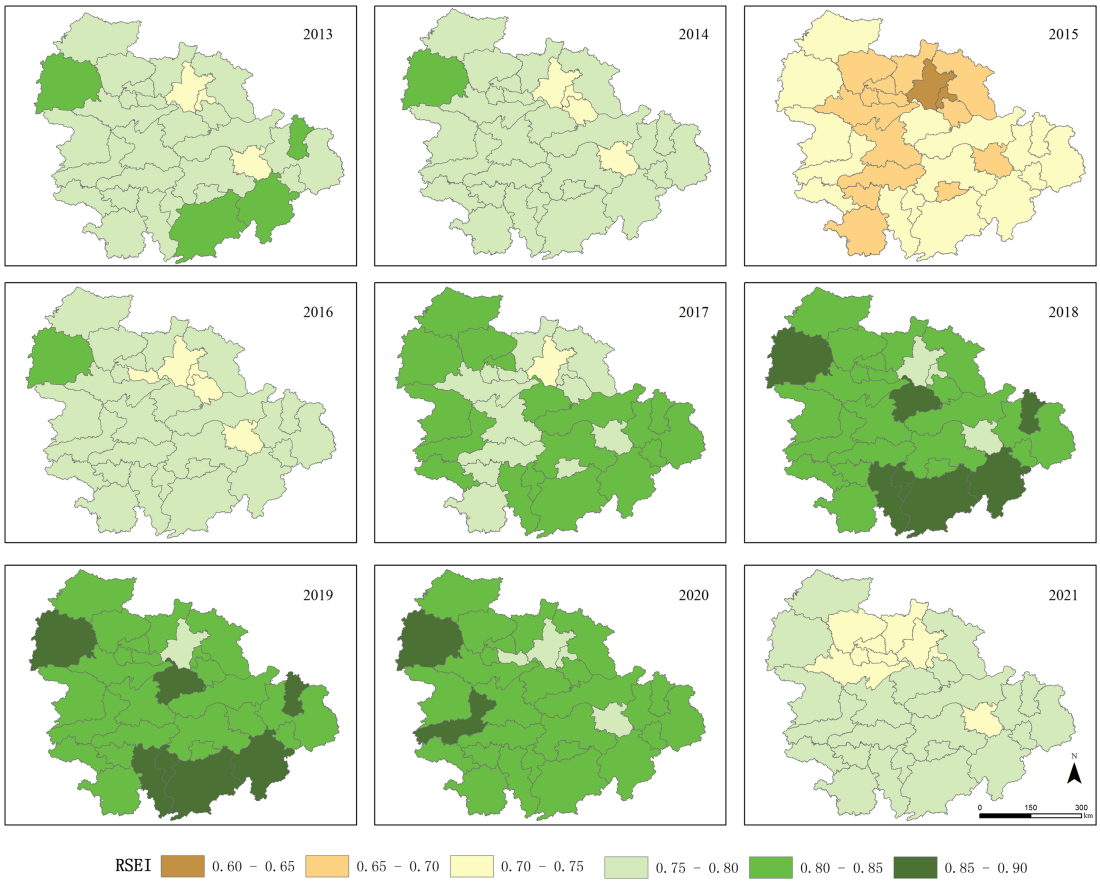

Fig. 5. RSEI distribution in UAMRYR from 2013 to 2021.

cities are expected to play a leading role for the surrounding cities.

Type 2: Peripheral Cities with Rapid Urbanization, these cities are closely linked to the central city and have experienced a faster urbanization process. They enter a higher stage of coordinated development earlier. Examples include Huangshi, known as the "deputy center of Wuhan City Circle" around Wuhan, Xiaogan, considered part of the "Wuhan New City," Ezhou, known as a "Satellite City," and Xiangtan and Zhuzhou in the vicinity of Changsha. These cities are expected to maintain their links with the central citis and keep up with its pace of development.

Type 3: Marginal Cities with Slow Urbanization, these cities are situated far away from the central cities and have undergone a slower urbanization process. Examples include Jingmen in Hubei Province, Hengyang in Hunan Province, and Ji'an in Jiangxi Province. They are located on the periphery of the urban agglomeration and face relatively limited resource allocation, leading to slower urban development. These cities need to strengthen their links with neighboring cities and develop their own special industries.

Type 4: Cities with Mismatched Development and Location, this category includes cities like Xiangyang and Jingdezhen, located on the fringe of the city cluster but having entered a higher level of coordinated development earlier. Xiangyang benefits from its advantageous geographical location, well-developed transportation, rich history, and deep cultural heritage. It serves as a vice-center city of Hubei Province. Jingdezhen, known as the "Porcelain Capital," holds distinctions as China's first "National Strategic Emerging Industries Regional Agglomeration Development Pilot" and "National Innovative Industry Cluster Pilot." In addition, it boasts a thriving tourism industry. These cities need to continue to maintain the development of their distinctive industries and strengthen their ties with central cities.

Type 5: Cities Adjacent to Central Cities with Poor Coordination, this group includes Shangrao, neighboring Nanchang, and Yiyang, adjacent to Changsha. These cities, situated on the fringes of urban agglomerations, face challenges in achieving coordination. They require strengthening efforts to accelerate regional integration and facilitate the free flow of resources, human capital, and technology.

2) Dynamic Coupling Coordination Degree Analysis: To more accurately depict the level of urban development within the UAMRYR, this study employs a dynamic coupling model to illustrate the evolving dynamics of the EEQ and urbanization in the city cluster. Table II shows the dynamic coupling coordination degree of the three provincial capitals from 2013 to 2021.

The evolution of the three provincial capitals can be broadly categorized into two stages: 1) 2013–2014: Low-Level Coordination (Fourth Quadrant)–During this period, the coordinated coupling of urbanization and the EEQ was situated in the fourth

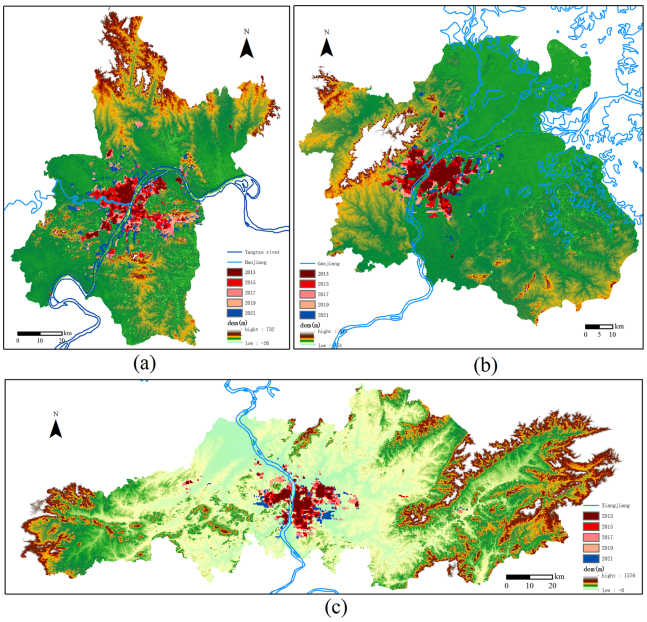

Fig. 6. Built-up area boundaries of the provincial capital city each year from 2013 to 2021. (a) Wuhan. (b) Nanchang. (c) Changsha.

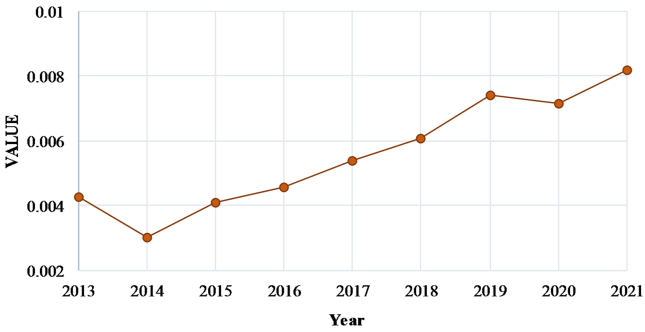

Fig. 7. CNLI changes of UAMRYR from 2013 to 2021.

TABLE II
DYNAMIC COUPLING COORDINATION DEGREE OF THREE PROVINCIAL CAPITAL CITIES FROM 2013 TO 2021

	Wuhan	Changsha	Nanchang
2013	-82.26°	-74.30°	-88.05°
2014	-88.96°	-87.74°	-88.35°
2015	67.93°	58.27°	79.28°
2016	84.34°	82.07°	87.02°
2017	87.37°	86.19°	88.37°
2018	88.80°	87.90°	89.09°
2019	89.47°	88.60°	89.48°
2020	89.77°	88.88°	89.68°
2021	89.92°	88.98°	89.80°

quadrant, indicating a state of low-level coordination. Urbanization was in a phase of rapid expansion, accompanied by a decline in EEQ. The coordinated coupling between these two factors deteriorated during this phase. 2) 2015–2021: Coordinated Development (First Quadrant)—From 2015 onward, the coordinated coupling of urbanization and ecology shifted to the first quadrant, signifying a stage of coordinated development. The year 2015 served as a transitional period characterized by ecological degradation resulting from rapid city construction. However, in 2016, with the official issuance of the outline of the development plan, ecological investments were made, leading to an improvement in EEQ. Simultaneously, urbanization continued to advance rapidly, with a substantial increase in the coordinated coupling of the city, nearing the 90° mark. This indicates an impending period of rapid development, where the overall coordinated development system is on the verge of entering an extreme development stage. During this phase, the resource and EEQ crisis enters a latent period. This analysis underscores that in the early stages of urbanization, a certain degree of ecological damage is often incurred as a necessary cost. However, as urbanization progresses, the EEQ is expected to ameliorate in tandem with urban development.

IV. DISCUSSION

A. Changes in the Ecological Quality of the Expanded Built-Up Area

To investigate the factors contributing to the increasing coordination between ecological quality and economic development in cities undergoing accelerated urbanization, this study analyzed the distribution of RSEI within the built-up areas of the three provincial capitals. Fig. 12 illustrates the distribution of RSEI within these areas, revealing similar patterns. As cities expanded, the distribution of EEQ within the built-up areas underwent the following evolution: 1) Early Stage of Rapid Urbanization (2013–2015). During this phase, the ecological quality within the built-up areas primarily experienced deterioration. 2) Post-2016 Sustainable Development. After 2016, when urban development increasingly emphasized sustainability, the ecological quality within the built-up areas began to improve. The distribution of RSEIs gradually shifted toward higher grades.

These changes in the EEQ within the built-up areas mirror the complex interplay between urbanization and the EEQ. Rapid city construction initially resulted in short-term ecological damage. However, as urbanization advanced, investments in EEQ protection increased. Numerous urban greening projects, including pocket parks, riverside parks, lake parks, community greening, and road greening, were implemented. These initiatives not only enhanced the aesthetics of the city, but also effectively addressed the demand for green space in densely populated urban areas. In addition, they mitigated the urban heat island effect and relieved ecological pressures to some extent. The analysis also considered the green space ratio within the built-up areas of the three provincial capital cities, as sourced from annual statistical yearbooks (see Table III). Wuhan and Changsha exhibited a consistent upward trend in their green space ratios within built-up areas. In contrast, Nanchang's green space ratio fluctuated but remained relatively stable. The rising green space ratios suggest a more positive relationship between urban development and the EEQ.

However, it is important to note that the overall trend in RSEI for the entire region and the distribution of RSEI within the

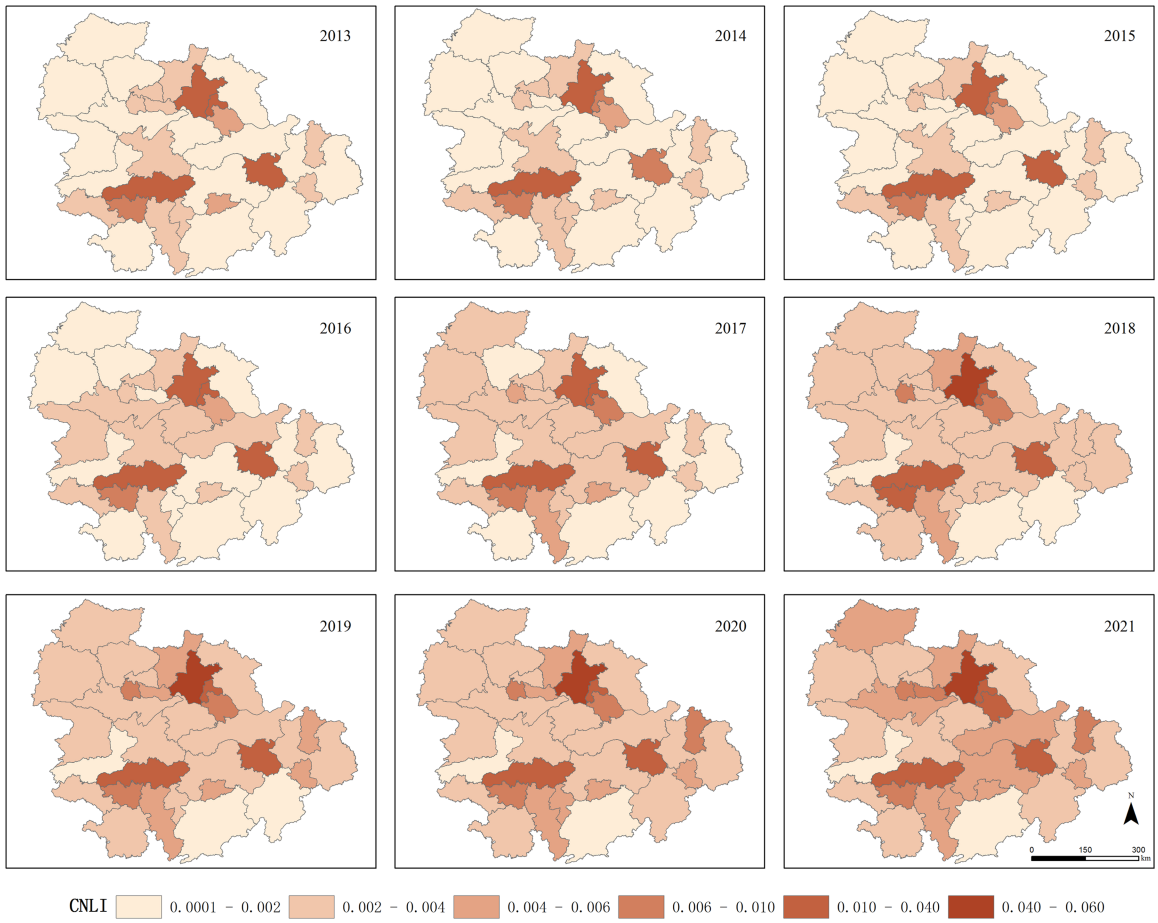

Fig. 8. CNLI distribution in UAMRYR from 2013 to 2021.

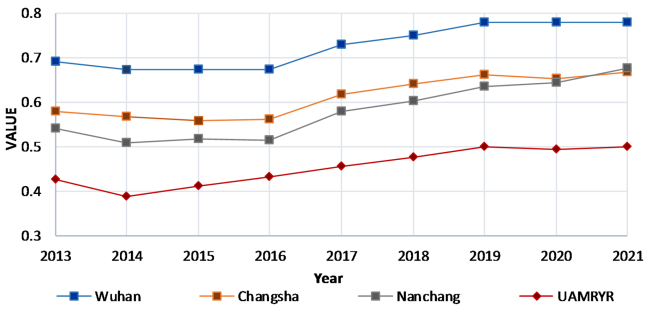

Fig. 9. Coupling coordination degree changes from 2013 to 2021.

TABLE III
GREEN SPACE RATIO IN BUILT-UP AREAS OF THREE PROVINCIAL CAPITAL CITIES FROM 2013 TO 2021 (%)

	Wuhan	Changsha	Nanchang
2013	32.94	33.43	40.09
2014	33.80	34.53	40.01
2015	34.19	33.90	38.90
2016	34.18	34.63	38.70
2017	34.47	35.11	39.87
2018	35.37	35.17	40.62
2019	35.74	35.25	39.30
2020	37.05	33.40	39.31
2021	40.02	40.85	40.00

built-up areas also indicate a deterioration in ecological conditions from 2020 onward. Upon examining the contributions of individual factors, it becomes apparent that LST has played an increasingly negative role from 2020, with its contribution worsening from −0.13 in 2019 to −0.24 in 2021. Furthermore, the expansion of the built-up area has continued to grow each year, contributing to a gradual decline in RSEI values from 2020 onward. Upon reviewing climate bulletins and related information, it was discovered that 2021 marked the highest national average temperature recorded since 1951, accompanied by frequent extreme weather and climate events, including heavy precipitation. In response to the threats posed by such extreme weather events, it is imperative to establish a strategic, targeted, and instructive planning system for resilient cities. This should involve the enhancement of urban infrastructure and facilities to promote the development of resilient cities capable of effectively addressing and mitigating the impacts of extreme weather disasters.

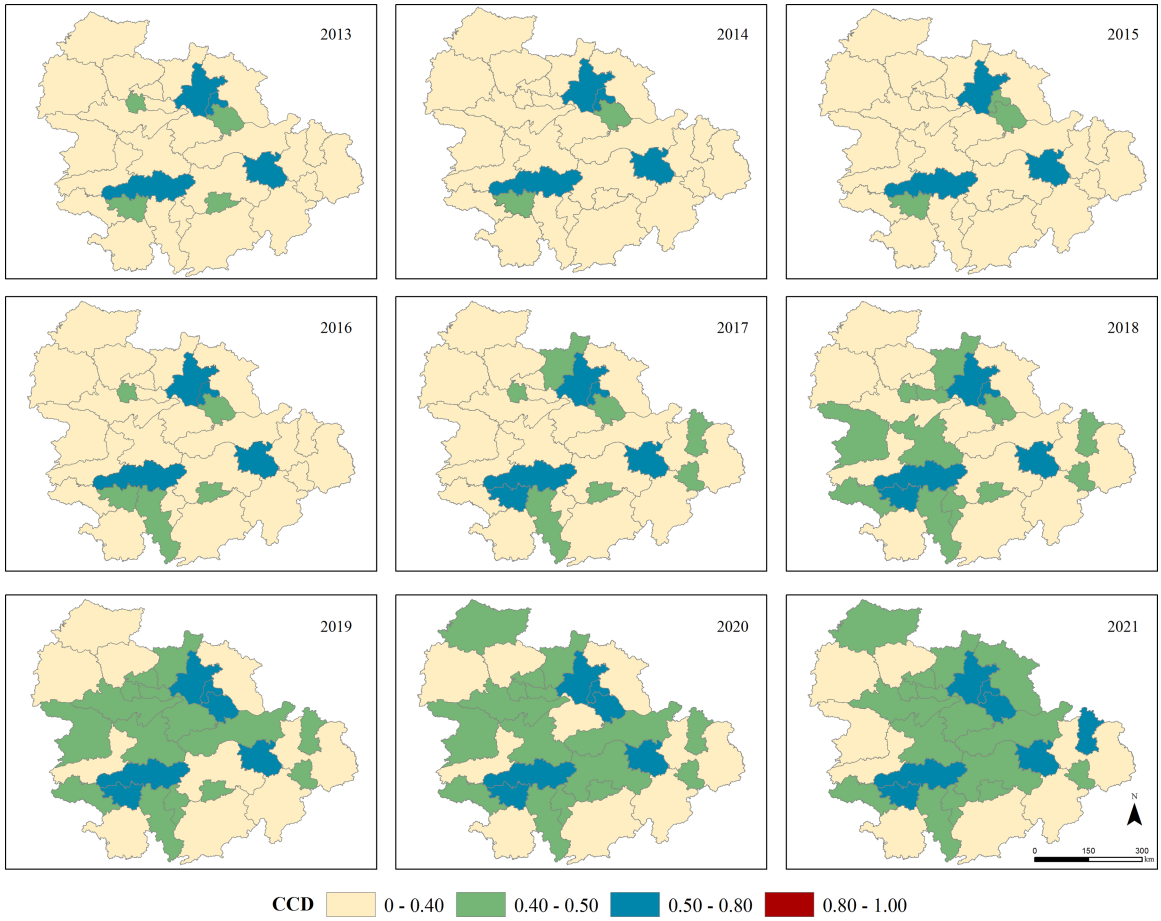

Fig. 10. Coupling coordination degree distribution in UAMRYR from 2013 to 2021.

B. Challenges Encountered in the Development of UAMRYR

Based on the results of the coupling analysis, two main challenges in the development of UAMRYR are evident

1) Uneven Development: The analysis reveals a significant disparity in development within the region. The urbanization process and degree of coupling coordination of the three central cities (Wuhan, Changsha, and Nanchang) are substantially higher than those of most other cities in the cluster. Notably, the development of urban clusters around Wuhan in Hubei Province displays a pattern of "one strong and many weak." To address this, the Wuhan metropolitan area should establish strong connections with adjacent areas to foster a more balanced and healthy development of the entire city cluster. In the Changsha–Zhuzhou–Xiangtan city group in Hunan Province, while Changsha stands as a prominent city with a developed central business district and high-tech industrial parks, Zhuzhou serves as a vital railway hub with a strong heavy industrial base, and Xiangtan boasts historical significance and resources in mining and iron and steel industries. However, the overall development of these cities is not as robust as the central cities in other clusters. To enhance development, the Changsha–Zhuzhou–Xiangtan city group should maintain Changsha as the primary core, with Zhuzhou and Xiangtan as sub-cores, leading the development of other cities within the cluster. The development level of clusters around Poyang Lake in Jiangxi Province is relatively low, with the core city Nanchang experiencing slower growth. The cities in this cluster exhibit similarities in resource endowments and transportation conditions, but their development strength remains weak. In the long term, these clusters should engage in comprehensive planning, focusing on the integration of urban and rural economies, with an emphasis on creating an ecological city cluster. This approach positions the cluster to become a crucial pivot point for connecting with the Pearl River Delta and Yangtze River Delta regions.

2) Poor Regional Connectivity: The analysis highlights a challenge related to poor regional connectivity. Peripheral cities of the three major metropolitan areas consistently displayed lower levels of coordinated development compared to cities closer to the central urban areas. It wasn't until 2020 that the degree of coordinated development among these peripheral cities caught up with that of their counterparts. To address this issue, future development efforts in the three major city clusters should prioritize preventing marginalization of peripheral cities. They should seek to drive integration among adjacent cities, reducing disparities in city scale and strengthening connectivity between cities.

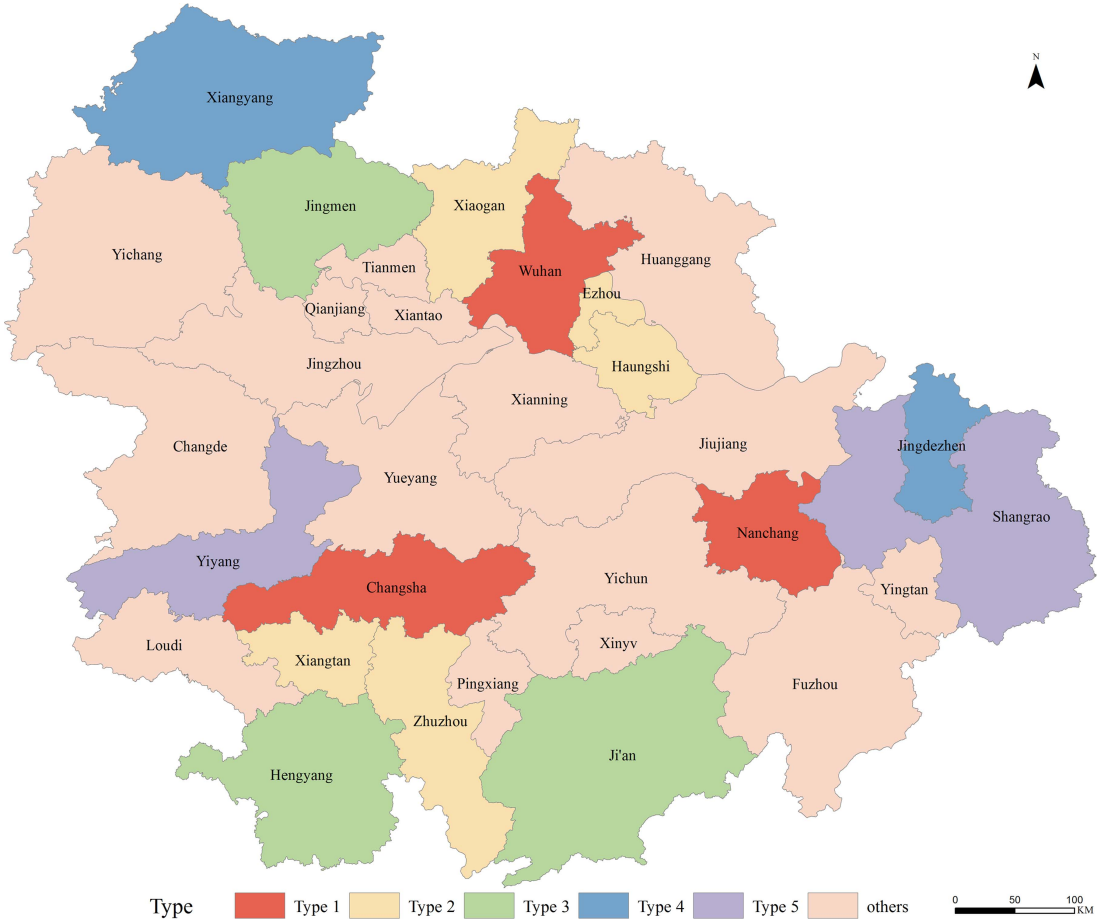

Fig. 11. Classification of city types.

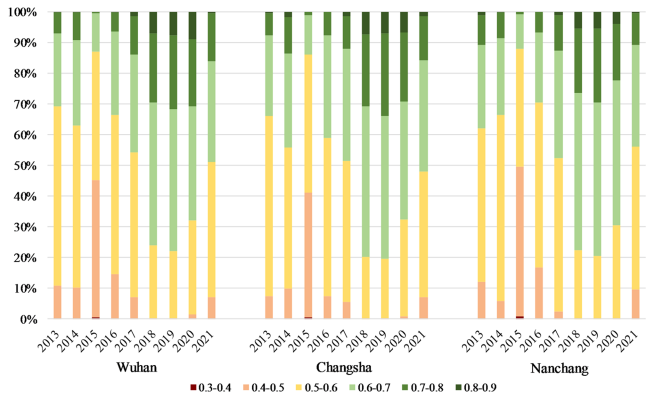

Fig. 12. Distribution of RSEI in built-up areas from 2013 to 2021 in three provincial capitals.

C. Limitations and Future Works

1) Data Source: In the process of calculating the RSEI using the GEE platform, obtaining a complete Landsat 8 image for the expansive study area posed challenges. To address this, we opted to select the median values from June to September during the vegetation growing season and applied temporal interpolation techniques to generate a more comprehensive image of the study area. However, it is worth noting that there are still areas with missing data. As part of future research, we may explore the use of multisource data fusion methods to further enhance the completeness of our study area images.

2) Nighttime Light Data Processing: During the data preprocessing of NPP/VIIRS remote sensing images, we employed a method of selecting the value at the 99.9th percentile as the maximum threshold for noise removal. Subsequent calculations revealed that all lighting index values were relatively small. While these values have minimal impact on our subsequent analyses, we will consider exploring normalization of the lighting index or alternative threshold selection methods in future research.

3) Scope of the Study: The YRB encompasses three major urban agglomerations: the Yangtze River Delta urban agglomeration, the urban agglomeration in the middle reaches of the Yangtze River, and the Chengdu–Chongqing urban agglomeration. This study primarily focuses on analyzing the relationship between ecological quality and the urbanization process within the urban agglomeration in the middle reaches of the Yangtze River. In future studies, we plan to expand our analysis to encompass all three urban agglomerations, allowing for a comprehensive comparative analysis. This broader perspective will provide insights into the coordinated development status of the entire YRB.

V. Conclusion

In this study, we first utilized the RSEI and the CNLI to assess the EEQ and urbanization process in UAMRYR from 2013 to 2021. Afterward, we analyzed the degree of coordination of the coupled development of UAMRYR based on these two indices and studied the stages of urban dynamic development of the central city. And based on the results, we classified the types of cities in UAMRYR and analyzed the challenges to the development of this urban agglomeration. These analyses are of significant importance for urbanization decision-making and optimizing the EEQ. The key findings of this study are as follows:

1) From 2013 to 2021, the overall ecological quality in UAMRYR exhibited a pattern of initial decline followed by fluctuations. Notably, the EEQ of central cities is generally lower than that of other cities.
2) Over the same period, the average level of urbanization in UAMRYR steadily increased. The urbanization level of provincial capital cities is significantly higher than that of other cities, and the urbanization process gradually radiates from provincial capital cities to peripheral cities.
3) The coupling coordination degree in UAMRYR experienced a brief decline followed by continuous growth to stability from 2013 to 2021. The three provincial capital cities consistently maintained a highly coordinated coupling state. By 2021, most cities had transitioned from a low level of coordinated coupling to a moderately coordinated coupling state. During the same period, the urban dynamic development stage of the three provincial capital cities entered the coordinated development stage from the low-level coordination stage in 2015. This shift signified the onset of a rapid development phase, and the entire coordinated development system was on the cusp of entering an extreme development stage.
4) Cities in UAMRYR can be categorized into five types based on coupled development. And the main challenges faced by URMRYR are uneven development and poor regional connectivity.

References

[1] Y. Bai, X. Deng, S. Jiang, Q. Zhang, and Z. Wang, "Exploring the relationship between urbanization and urban eco-efficiency: Evidence from prefecture-level cities in China," *J. Cleaner Prod.*, vol. 195, pp. 1487–1496, Sep. 2018, doi: 10.1016/j.jclepro.2017.11.115.

[2] X. Zheng and T. Chen, "High spatial resolution remote sensing image segmentation based on the multiclassification model and the binary classification model," *Neural Comput. Appl.*, vol. 35, no. 5, pp. 3597–3604, Jan. 2023, doi: 10.1007/s00521-020-05561-8.

[3] H. Cai, T. Chen, R. Niu, and A. Plaza, "Landslide detection using densely connected convolutional networks and environmental conditions," *IEEE J. Sel. Topics Appl. Earth Observ. Remote Sens.*, vol. 14, pp. 5235–5247, May 2021, doi: 10.1109/JSTARS.2021.3079196.

[4] A. Elmes, J. Rogan, C. Williams, S. Ratick, D. Nowak, and D. Martin, "Effects of urban tree canopy loss on land surface temperature magnitude and timing," *ISPRS J. Photogrammetry Remote Sens.*, vol. 128, pp. 338–353, Jun. 2017, doi: 10.1016/j.isprsjprs.2017.04.011.

[5] M. J. McDonnell and I. MacGregor-Fors, "The ecological future of cities," *Science*, vol. 352, no. 6288, pp. 936–938, May 2016, doi: 10.1126/science.aaf3630.

[6] D. Ghosh, S. Chakravortty, A. Plaza, and J. Li, "Change prediction and modeling of dynamic mangrove ecosystem using remotely sensed hyperspectral image data," *J. Appl. Remote Sens.*, vol. 15, no. 4, pp. 189–211, Sep. 2021, doi: 10.1117/1.JRS.15.042606.

[7] Y. Song, "Ecological city and urban sustainable development," *Procedia Eng.*, vol. 21, pp. 142–146, Dec. 2011, doi: 10.1016/j.proeng.2011.11.1997.

[8] M. Cao et al., "Multi-scenario simulation of land use for sustainable development goals," *IEEE J. Sel. Topics Appl. Earth Observ. Remote Sens.*, vol. 15, pp. 2119–2127, Feb. 2022, doi: 10.1109/JSTARS.2022.3152904.

[9] G. C. Spyropoulos, P. T. Nastos, and K. P. Moustris, "Performance of aether low-cost sensor device for air pollution measurements in urban environments. Accuracy evaluation applying the air quality index (AQI)," *Atmosphere*, vol. 12, no. 10, Sep. 2021, Art. no. 1246, doi: 10.3390/atmos12101246.

[10] A. Tyagi, S. Arya, A. Nandan, and P. Mondal, "Assessment of groundwater using water quality index (WQI) at Saharanpur City, Uttar Pradesh (West), India," in *Proc. Int. Conf. Adv. Innovations Recycling Eng.*, 2023, vol. 301, pp. 1–10, doi: 10.1007/978-981-19-7506-6_1.

[11] E. A. Fano, M. Mistri, and R. Rossi, "The ecofunctional quality index (EQI): A new tool for assessing lagoonal ecosystem impairment," *Estuarine, Coastal Shelf Sci.*, vol. 56, no. 3, pp. 709–716, May 2003, doi: 10.1016/S0272-7714(02)00289-5.

[12] X. Liao, W. Li, and J. Hou, "Application of GIS based ecological vulnerability evaluation in environmental impact assessment of master plan of coal mining area," *Procedia Environ. Sci.*, vol. 18, pp. 271–276, Jun. 2013, doi: 10.1016/j.proenv.2013.04.035.

[13] H. Jianxin and W. Dongying, "Research on the comprehensive evaluation system for river in jiangsu province coastal areas," *Procedia - Social Behav. Sci.*, vol. 96, pp. 1025–1029, Nov. 2013, doi: 10.1016/j.sbspro.2013.08.117.

[14] S. Park, F. Kazama, and S. Lee, "Assessment of water quality using multivariate statistical techniques: A case study of the Nakdong river basin, Korea," *Environ. Eng. Res.*, vol. 19, no. 3, pp. 197–203, Sep. 2014, doi: 10.4491/eer.2014.008.

[15] Y. Chen et al., "Bird community structure is driven by urbanization level, blue-green infrastructure configuration and precision farming in Taizhou, China," *Sci. Total Environ.*, vol. 859, Feb. 2023, Art. no. 160096, doi: 10.1016/j.scitotenv.2022.160096.

[16] C. Wang et al., "Spatial heterogeneity of urbanization impacts on ecosystem services in the urban agglomerations along the Yellow River, China," *Ecol. Eng.*, vol. 182, Sep. 2022, Art. no. 106717, doi: 10.1016/j.ecoleng.2022.106717.

[17] W. W. Hanlon and S. Heblich, "History and urban economics," *Regional Sci. Urban Econ.*, vol. 94, 2022, Art. no. 103751, doi: 10.1016/j.regsciurbeco.2021.103751.

[18] M. Maldet, G. Lettner, C. Loschan, D. Schwabeneder, and H. Auer, "Creating an indicator system for the United Nations Sustainable Development Goals in communities and municipalities: Application and analysis in an Austrian case study," *Heliyon*, vol. 9, no. 8, Sep. 2023, Art. no. e19010, doi: 10.1016/j.heliyon.2023.e19010.

[19] H. Xu, "A remote sensing index for assessment of regional ecological changes," *China Environ. Sci.*, vol. 33, no. 05, pp. 889–897, Jun. 2013.

[20] L. Zhuo, P. Shi, J. Chen, and T. Ichinose, "Application of compound night light index derived from DMSP/OLS data to urbanization analysis in China in the 1990s," *Acta Geographica Sinica*, vol. 58, no. 6, pp. 893–902, 2003, doi: 10.11821/xb200306013.

[21] K. E. Boulding, "Steady-state economics: Second edition with new essays: Herman E. Daly. Island Press, Washington, DC, 1991, 302 pp., ISBN 1 55963 072 8," *Ecol. Econ.*, vol. 7, no. 2, pp. 179–180, 1993, doi: 10.1016/0921-8009(93)90055-B.

[22] N. Caill-Milly, J. B. Garmendia, F. D'Amico, O. Guyader, C. Dang, and N. Bru, "Adapting a dynamic system model using life traits and local fishery knowledge — Application to a population of exploited marine bivalves (Ruditapes philippinarum) in a mesotidal coastal lagoon," *Ecol. Model.*, vol. 470, Aug. 2022, Art. no. 110034, doi: 10.1016/j.ecolmodel.2022.110034.

[23] T. Panayotou, "Demystifying the environmental Kuznets curve: Turning a black box into a policy tool," *Environ. Develop. Econ.*, vol. 2, no. 4, pp. 465–484, Nov. 1997.

[24] L. P. Tan, "Bibliometrics of social entrepreneurship research: Cocitation and bibliographic coupling analyses," *Cogent Bus. Manag.*, vol. 9, no. 1, Sep. 2022, Art. no. 2124594, doi: 10.1080/23311975.2022.2124594.

[25] A. Müller, M. Riedl, T. Penzel, H. Bonnemeier, J. Kurths, and N. Wessel, "Coupling analysis of transient cardiovascular dynamics," *Biomedizinische Technik. Biomed. Eng.*, vol. 58, no. 2, pp. 131–139, Apr. 2013, doi: 10.1515/bmt-2012-0030.

[26] A. Mandal and D. Maity, "Seismic analysis of dam-foundation-reservoir coupled system using direct coupling method," *Coupled Syst. Mech.*, vol. 8, no. 5, pp. 393–414, 2019, doi: 10.12989/csm.Oct.2019,8.5.393.

[27] B. Qiao and C. Fang, "The dynamic coupling model of the harmonious development between urbaniza-tion and eco-environment and its application in arid area," *Acta Ecologica Sinica*, vol. 25, no. 11, pp. 211–217, Nov. 2005.
[28] Y. Liu, R. Li, and X. Song, "Analysis of coupling degrees of urbanization and ecological environment in China," *J. Natural Resour.*, vol. 20, no. 1, pp. 105–112, Nov. 2005, doi: 10.11849/zrzyxb.2005.01.015.
[29] X. Zhang et al., "Coupling coordination between the ecological environment and urbanization in the middle reaches of the Yangtze River urban agglomeration," *Urban Climate*, vol. 52, Sep. 2023, Art. no. 101698, doi: 10.1016/j.uclim.2023.101698.
[30] X. Yu, L. Wang, Q. Yang, and S. Ye, "Background of the Yangtze River Economic Belt development strategy and geography interpretation of its innovative development," *Prog. Geogr.*, vol. 34, no. 11, pp. 1368–1376, Sep. 2015, doi: 10.18306/dlkxjz.2015.11.004.
[31] W. Tan, L. Tian, H. Shen., and C. Zeng, "A new downscaling-calibration procedure for TRMM precipitation data over Yangtze River economic belt region based on a multivariate adaptive regression spline model," *IEEE Trans. Geosci. Remote Sens.*, vol. 60, Jun. 2022, Art. no. 4702819, doi: 10.1109/TGRS.2021.3087896.
[32] H. Xu, "A study on information extraction of water body with the modified normalized difference water index," *J. Remote Sens.*, vol. 9, no. 5, pp. 589–595, Sep. 2005, doi: 10.11834/jrs.20050586.
[33] J. Chen. and L. Li, "Regional economic activity derived from MODIS data: A comparison with DMSP/OLS and NPP/VIIRS nighttime light data," *IEEE J. Sel. Topics Appl. Earth Observ. Remote Sens.*, vol. 12, no. 8, pp. 3067–3077, Aug. 2019, doi: 10.1109/JSTARS.2019.2915646.
[34] X. Ma, X. Tong, S. Liu, C. Li, and Z. Ma, "A multisource remotely sensed data oriented method for 'Ghost City' phenomenon identification," *IEEE J. Sel. Topics Appl. Earth Observ. Remote Sens.*, vol. 11, no. 7, pp. 2310–2319, Jul. 2018, doi: 10.1109/JSTARS.2018.2824302.
[35] Z. Chen, B. Yu, Y. Hu, C. Huang, K. Shi, and J. Wu, "Estimating house vacancy rate in metropolitan areas using NPP-VIIRS nighttime light composite data," *IEEE J. Sel. Topics Appl. Earth Observ. Remote Sens.*, vol. 8, no. 5, pp. 2188–2197, May 2015, doi: 10.1109/JSTARS.2015.2418201.
[36] Z. Tong, X. Li, and H. Cao, "Comparing DMSP/OLS stable nighttime light with radiance calibrated nighttime light," *IEEE J. Sel. Topics Appl. Earth Observ. Remote Sens.*, vol. 14, pp. 11116–11125, Oct. 2021, doi: 10.1109/JSTARS.2021.3123065.
[37] N. Zhao, Y. Zhou, and E. L. Samson, "Correcting incompatible DN values and geometric errors in nighttime lights time-series images," *IEEE Trans. Geosci. Remote Sens.*, vol. 53, no. 4, pp. 2039–2049, Apr. 2015, doi: 10.1109/TGRS.2014.2352598.
[38] M. Li and W. Cai, "Calibration for multi-temporal NPP/VIIRS nighttime light remote sensing images," *Bull. Surveying Mapping*, no. 07, pp. 122–126, Jul. 2019, doi: 10.13474/j.cnki.11-2246.2019.0233.
[39] C. Li, J. Yang, and Y. Zhang, "Evaluation and analysis of the impact of coastal urban impervious surfaces on ecological environments," *IEEE J. Sel. Topics Appl. Earth Observ. Remote Sens.*, vol. 16, pp. 8721–8733, Aug. 2023, doi: 10.1109/JSTARS.2023.3310616.
[40] Z. Wang, T. Chen, D. Zhu, K. Jia, and A. Plaza, "RSEIFE: A new remote sensing ecological index for simulating the land surface eco-environment.," *J. Environ. Manage.*, vol. 326, Jan. 2023, doi: 10.1016/j.jenvman.2022.116851.
[41] X. Hang et al., "Land surface eco-environmental situation index (LSEESI) derived from remote sensing," *IEEE Trans. Geosci. Remote Sens.*, vol. 61, Sep. 2023, Art. no. 4408018, doi: 10.1109/TGRS.2023.3311469.
[42] D. Zhu, T. Chen, Z. Wang, and R. Niu, "Detecting ecological spatial-temporal changes by remote sensing ecological index with local adaptability," *J. Environ. Manage.*, vol. 299, Dec. 2021, Art. no. 113655, doi: 10.1016/j.jenvman.2021.113655.
[43] S. Wang, W. Kong, L. Ren, D. Zhi, and B. Dai, "Research on misuses and modification of coupling coordination degree model in China," *J. Natural Resour.*, vol. 36, no. 03, pp. 793–810, Jan. 2021, doi: 10.31497/zrzyxb.20210319.
[44] C. Wang and N. Tang, "Spatio-temporal characteristics and evolution of rural production-living-ecological space function coupling coordination in Chongqing municipality," *Geogr. Res.*, vol. 37, no. 06, pp. 1100–1114, 2018, doi: 10.11821/dlyj201806004.
[45] C. He et al., "Reconstructing the spatial process of urbanization in mainland China in the 1990s based on DMSP/OLS nighttime lighting data and statistical data," *Chin. Sci. Bull.*, vol. 51, no. 07, pp. 856–861, Apr. 2006, doi: 10.1360/972004-300.

Can Li received the B.S. degree in geographic information science from Yangtze University, Wuhan, China, in 2021. She is currently working toward the M.S. degree in resources and environment with China University of Geosciences, Wuhan, China.

Her current main research interest is remote sensing-based monitoring of urban ecosystem quality.

Tao Chen (Senior Member, IEEE) received the Ph.D. degree in photogrammetry and remote sensing from Wuhan University, Wuhan China, in 2008.

He is currently an Associate Professor with the School of Geophysics and Geomatics, China University of Geosciences, Wuhan, China. He has authored or coauthored more than 60 scientific papers including IEEE TRANSACTIONS ON GEOSCIENCE AND REMOTE SENSING, IEEE JOURNAL OF SELECTED TOPICS IN APPLIED EARTH OBSERVATIONS AND REMOTE SENSING, *International Journal of Applied Earth Observation and Geoinformation*, etc., and guest edited ten journal special issues. From 2015 to 2016, he was a Visiting Scholar with the University of New South Wales, Sydney, NSW, Australia. His research interests include image processing, machine learning, and geological remote sensing.

Dr. Chen serves as the Associate Editor for the IEEE JOURNAL OF SELECTED TOPICS IN APPLIED EARTH OBSERVATIONS AND REMOTE SENSING.

Kun Jia received the B.S. degree in surveying and mapping engineering from Central South University, Changsha, China, in 2006, the Ph.D. degree in cartography and GIS from the Institute of Remote Sensing Applications, Chinese Academy of Sciences, Beijing, China, in 2011.

He is currently a Full Professor with the State Key Laboratory of Remote Sensing Science and also the Beijing Engineering Research Center for Global Land Remote Sensing Products, Faculty of Geographical Science, Beijing Normal University, Beijing, China. His main research interests include estimation of vegetation parameters, land cover classification, and agriculture monitoring using remote sensing data.

Antonio Plaza (Fellow, IEEE) received the M.Sc. and Ph.D. degrees in computer engineering from the Department of Technology of Computers and Communications, University of Extremadura, Badajoz, Spain, in 1999 and 2002, respectively.

He is currently a Full Professor and the Head of the Hyperspectral Computing Laboratory, Department of Technology of Computers and Communications, University of Extremadura. He has authored more than 600 publications and guest edited ten journal special issues. He has reviewed more than 500 manuscripts for more than 50 different journals.

Dr. Plaza served as the Editor-in-Chief for IEEE TRANSACTIONS ON GEOSCIENCE AND REMOTE SENSING from 2013 to 2017. He is included the Highly Cited Researchers List (Clarivate Analytics) from 2018 to 2020.